

# Solvent Remodeling in Single-Chain Amphiphilic Heteropolymer Systems

*Shayna L. Hilburg<sup>†</sup>, Alfredo Alexander-Katz<sup>†,\*</sup>*

<sup>†</sup>Department of Materials Science and Engineering, Massachusetts Institute of Technology,  
Cambridge, Massachusetts 02139, USA

## **ABSTRACT**

Through molecular dynamics simulations, we demonstrate how single-chain nanoparticles (SCNPs) assembled via transient linkages in water can remodel in organic solvent. Methacrylate-based random heteropolymers (RHPs) have shown promise in an assortment of applications that harness their bio-inspired properties. While their molecular behavior has been broadly characterized in water, many newer applications include the use of organic solvent rather than bio-mimetic conditions in which the polymer assemblies, typically driven by the hydrophobic effect, are less well understood. Here, we examine a specific RHP system which forms compact globular morphologies in highly polar and non-polar environments while adopting extended conformations in solvents of intermediate polarity. We also demonstrate the pivotal role of electrostatic interactions between charge groups in low dielectric mediums. Finally, we compare high temperature anneal cycles to room temperature equilibrations to illuminate activation barriers to remodeling upon environmental changes.

19 **LETTER**

20 Single-chain nanoparticles (SCNPs) harness synthetic macromolecules as promising drug  
21 delivery systems, nanomedicines, catalysts, and more.<sup>1</sup> While many SCNPs rely on covalent or  
22 other strongly associating linkages to assemble, a promising subset of materials use reversible,  
23 dynamic associations in their assembly.<sup>2</sup> One of the simplest and most cost effective SCNP designs  
24 is the combination of moieties with varying interaction energies which use solvophobic effects as  
25 a driving force to assembly. Methacrylate-based random heteropolymers (RHPs) are one such  
26 system, which self-assembles into nano-scale particles containing single or few chains in water,  
27 and offers an exciting avenue for protein stabilization and mimicry, nanofiltration, and other  
28 promising applications.<sup>3-7</sup> Behavior of methacrylate-based designs in water have been studied  
29 most in depth, as many of their applications occur in aqueous environments.<sup>8,9</sup>

30 We previously studied a specific RHP design-space through molecular dynamics (MD)  
31 simulations and elucidated the resulting SCNP structure and dynamics.<sup>10</sup> The work demonstrated  
32 that while theories are helpful in understanding these polymer systems, the inclusion of specific  
33 chemistries is necessary for a full picture of the molecular behavior. While the work has been  
34 pivotal in gaining a mechanistic picture of how the RHPs behave in water, several potential  
35 applications occur in, or require processing steps performed in, other solvents. The compactness  
36 and mobility of chains in solvents with different affinities for the varied chemical substituents has  
37 been leveraged to control structures of resulting membranes, gels, and other nanomaterials.<sup>7,11,12</sup>  
38 Characterizing the relationship between polymer behavior and its solvent environment allows such  
39 methods to be applied predictably for a variety of polymer-solvent systems.

40 While covalently cross-linked SCNPs would not be considerably altered by the presence  
41 of organic solvent, we expect drastic changes in systems, including ours, driven by transient

42 linkages reliant upon solvent interactions to drive assembly. Amphiphilic synthetic polymer  
43 systems which form compact assemblies in water can adopt extended conformations in solvents  
44 of intermediate polarity, within which both hydrophobic and hydrophilic components energetically  
45 prefer the enthalpic contributions to solvation over the entropic restriction of compactification, or  
46 reverse micelles in solvents which invert typical aqueous behavior, leading hydrophilic  
47 components to invert together while hydrophobic moieties preferentially orient to an assembly's  
48 surface. This behavior has been experimentally observed for amphiphilic homopolymers with  
49 amphiphilic monomers,<sup>13,14</sup> as well as for heteropolymers with both hydrophobic and hydrophilic  
50 monomers, most well characterized for 2-component copolymer systems.<sup>15-19</sup> The specific  
51 intramolecular interactions dictate how each polymer will adapt, with some systems maintaining  
52 monomer contacts in organic media compared to aqueous solvent due to strong intrachain  
53 associations which persist in the new environment.<sup>19,20</sup>

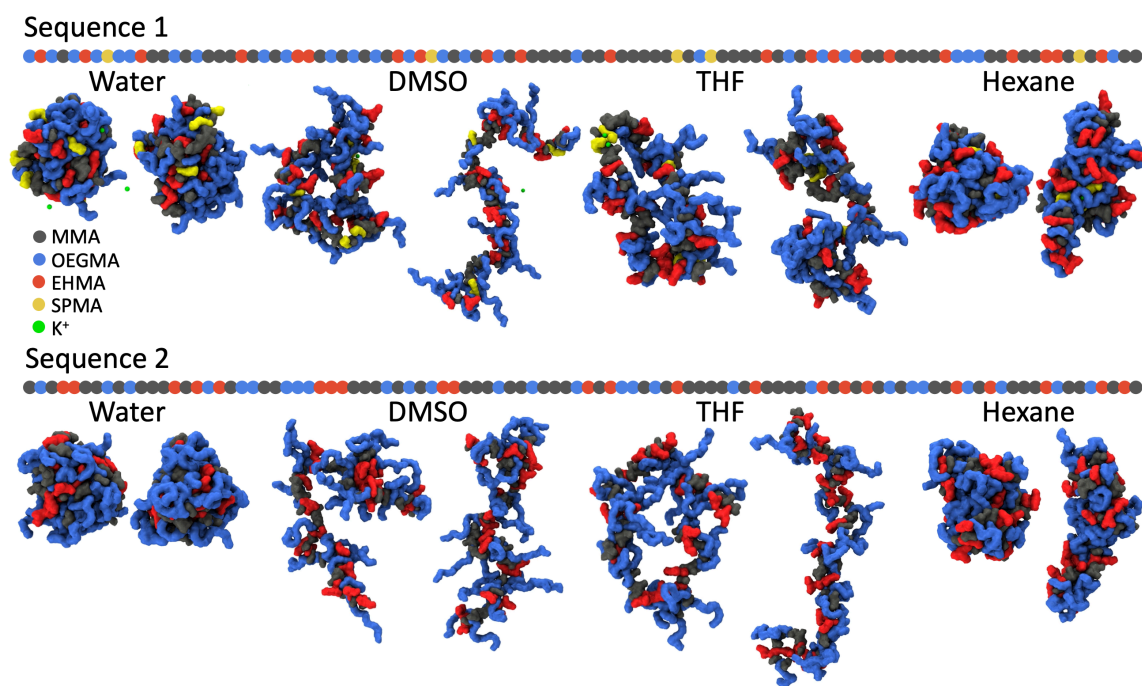
54 Our particular polymer of interest has been used to stabilize enzymes for the creation of  
55 sustainably degradable polyesters through solution-casting in toluene or dichloromethane.<sup>21</sup> In the  
56 current work, we leverage our previously demonstrated simulation methods and broaden them to  
57 a variety of organic solvents, namely tetrahydrofuran (THF), dimethyl sulfoxide (DMSO), and  
58 hexane. We use atomistic molecular dynamics (MD) simulations, having seen the importance of  
59 incorporating this level of chemical resolution through our prior work, as well as within the  
60 literature. While coarse-grained simulations have been useful for RHP systems, such as in  
61 demonstrating the correlation between stronger monomer interactions and smaller, denser  
62 nanoparticle formation in copolymers,<sup>22</sup> the methods require a fixed polarity and lack the atomic  
63 solvent structures, making inherently amphiphilic molecular substituents such as poly(ethylene  
64 glycol) difficult to model as they interact. Including chemical detail is vital to capturing the

65 configurational entropy for side chain reorientation when transferring solvents and maintaining  
66 separate assessment of backbone and side chain segments, which depending on their affinities to  
67 the solvent will greatly alter resulting morphologies.<sup>23,24</sup> In addition to our atomistic simulations of  
68 the four-component RHPs in water, atomistic resolution has been leveraged in simulating two-  
69 component amphiphilic copolymers in both water and chloroform.<sup>25</sup> We use similar techniques on  
70 our more complex system with more in-depth analysis and demonstrate the impact of added  
71 compositional complexity in a broader variety of solvents. The results we present show substantial  
72 differences in monomer accessibility and conformational flexibility which depend on solvent  
73 polarity and structure, as well as RHP chemistry. These behaviors affect how the molecules would  
74 interface during post-synthetic processing steps or at end application in non-aqueous solvents and,  
75 therefore, greatly impact their use. Beyond applications in organic solvent, our results also offer  
76 significant insight to potential interactions with other organic substances such as small molecules  
77 or hydrophobic biomacromolecules.

78         Herein, we explore RHP behavior using unbiased atomistic molecular dynamic methods  
79 with the Amber MD package, similar to our prior work.<sup>10,26</sup> Through a series of successive anneal  
80 cycles to 500 K in implicit water, ten conformations each of two distinct polymer sequences were  
81 created and then annealed to 650 K in explicit solvent: water, DMSO, THF, or hexane. The  
82 resulting single chain conformations at 300 K from these simulations were used for analysis.  
83 Equilibrated structures from explicit water were then transferred to DMSO, THF, or hexane for  
84 further study at room temperature as they adjust to the new solvent environments. Parameterization  
85 and simulation details are provided in the Supplementary Information.

86         The two random heteropolymer sequences investigated, Sequence 1 and Sequence 2 as shown  
87 in Figure 1, are composed of the methacrylate-based building blocks studied previously.<sup>10</sup>

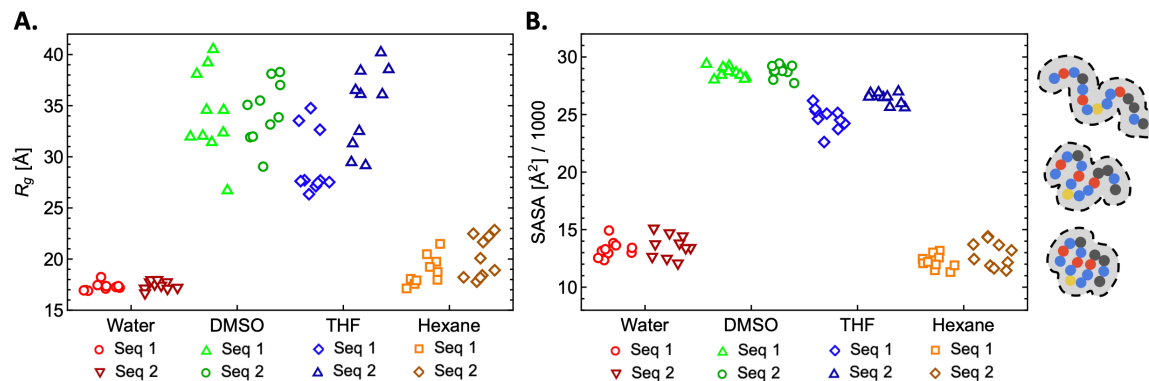
88 Sequence 1 contains all four monomer species—methyl methacrylate (MMA), oligo(ethylene  
89 glycol)methacrylate (OEGMA), 2-ethylhexyl methacrylate (EHMA), and 3-sulfopropyl  
90 methacrylate (SPMA)—used in the prior work, while Sequence 2 is similar but lacks the anionic  
91 SPMA monomer.



92  
93 Figure 1. Sequences and renderings of the conformations with the minimum (left) and maximum  
94 (right) mean radius of gyration for each system. Solvent is omitted for clarity.

95 Both sequences formed compact globular structures in water and hexane, with distinct  
96 surface compositions in each solvent apparent by visual inspection in Figure 1. DMSO and THF  
97 led to contrastingly extended conformations. Quantitatively, the mean radius of gyration ( $R_g$ ) and  
98 solvent accessible surface area (SASA) for each equilibrated conformation is presented in Figure  
99 2. The  $R_g$ , from which a minimum and maximum were selected for rendering in Figure 1, has a  
100 narrow distribution for compact structures in water and broader distributions for the organic  
101 solvents of interest. SASA, calculated in each solvent using Amber's default radius size to allow

102 cross-comparison, shows similar distributions within each dataset, indicating that the  
 103 configurations as adopted for the interaction energies between solvent and polymer have similar  
 104 amounts of contact despite entropically unique topologies indicated by unique  $R_g$  values. Sequence  
 105 1 and 2 have similar ranges for both properties in each examined environment, with the exception  
 106 of THF solvated structures which shows lower extension and solvation of sequence 1.

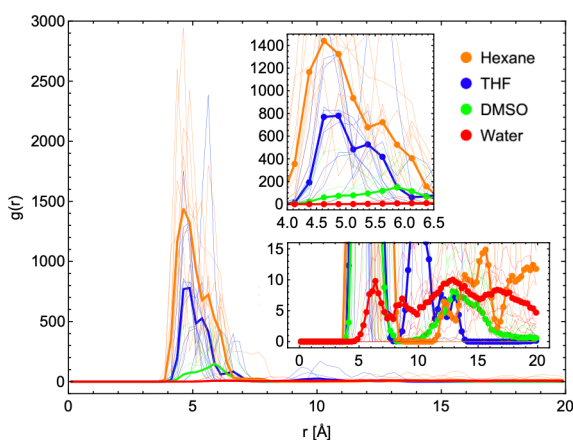


107  
 108 Figure 2. (A) Radius of gyration ( $R_g$ ) and (B) total solvent accessible surface area (SASA) with  
 109 schematic representation (right) of how conformation and accessible surface area relate. Results  
 110 represent the mean value from equilibrated structures after annealing in solvent of interest for each  
 111 conformation.

112 Mobility of the polymer backbone and side-chains generally scales with chain extension,  
 113 albeit with several notable trends by monomer type (Supplementary Figures 1-2). While mobility  
 114 in THF is high and mobility in hexane is low, corresponding to the compactness, low backbone  
 115 mobility in SPMA monomer residues lead to lower values for Sequence 1 as compared to Sequence  
 116 2. Mobility of the side-chains themselves are impacted by moiety sizes, with OEGMA consistently  
 117 having high fluctuations in all solvents due to its long side-chain length, as well as being soluble  
 118 in water, THF, and DMSO. As EHMA and SPMA have similar side chain lengths, their relative  
 119 side-chain mobilities are indicative, instead, of freedom of motion in the polymer configuration.

120 In water, SPMA fluctuates more than EHMA, while the trend is flipped in all three organic  
121 solvents. In hexane, SPMA is practically immobilized and EHMA has significantly higher  
122 fluctuations.

123 Polymer compactification and monomer mobilities all indicate that SPMA greatly impacts  
124 chain behavior. An assessment of the radial distribution function (RDF) between sulfur atoms in  
125 the SPMA's anionic sulfonate group, shown in Figure 3, shows that while some liquid-like features  
126 can be seen between SPMA moieties in water, increasingly pronounced features and short  
127 distances appear for the RHPs in DMSO, THF, and hexane. A similar analysis between sulfur and  
128 potassium counterions (Supplementary Figure 3) indicates that salt bridging leads to these effects.  
129 Intrachain associations have been observed in literature to restrict heteropolymer assembly through  
130 salt bridging in water amongst anionic and cationic monomers and in organic solvent via strong  
131 fluorocarbon associations.<sup>4,19</sup> The extremely high correlations between sulfur positions in THF and  
132 hexane in our conformations naturally explain the mobility and configurational differences  
133 between sequence 1 and 2, locking sequence 1 into place due to electrostatic interactions in the  
134 low dielectric mediums.

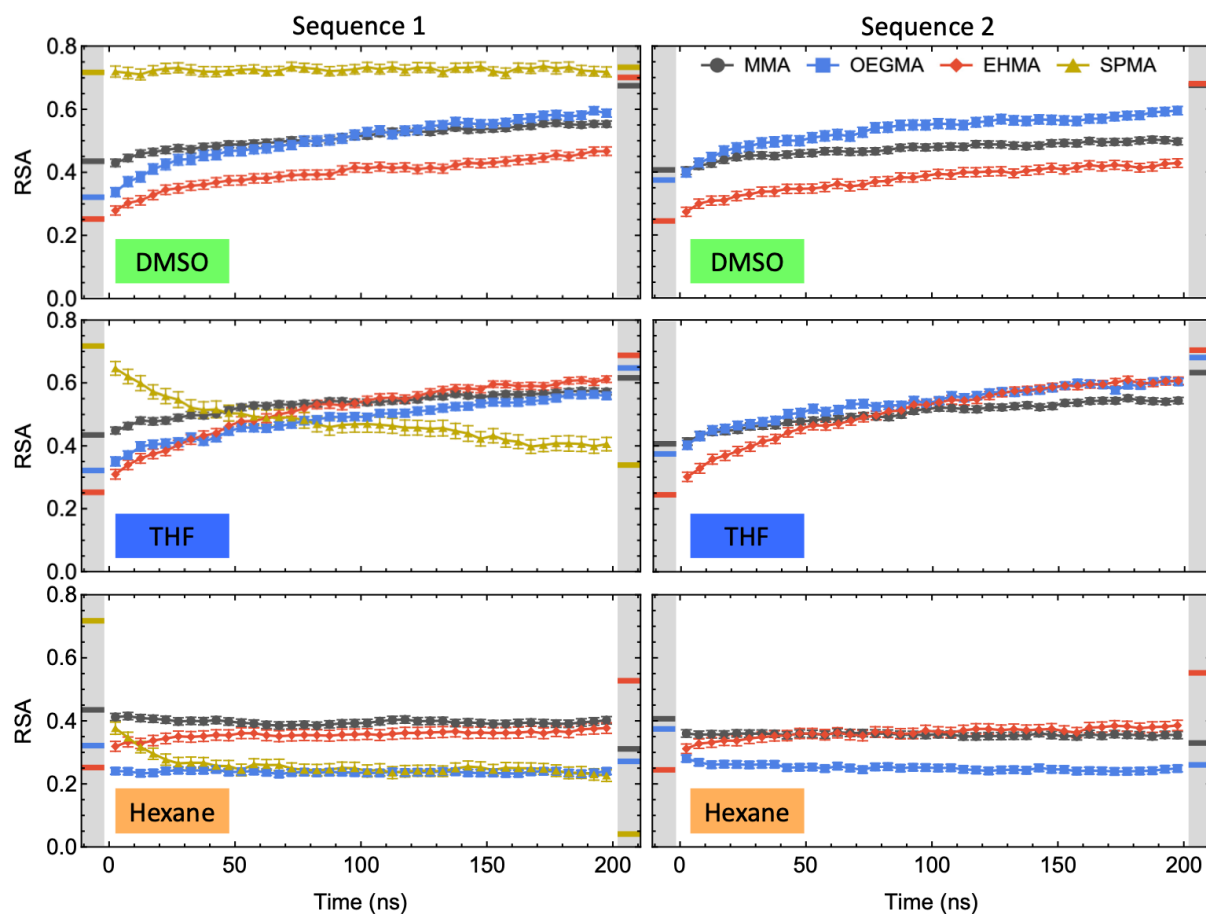


135

136 Figure 3. Radial distribution function of anionic moieties as measured between sulfur atoms within  
137 the sulfonate groups of SPMA monomers. Bold lines show mean values over ten conformations  
138 (each shown as thin lines) for the equilibrated sequence as annealed in each solvent of interest.

139 With equilibrated structures characterized, we turn to the transformation from water to  
140 organic solvent. Data presented thus far annealed polymer chains in the explicit solvent of interest  
141 before equilibrating for 60ns at 300 K, of which the final 40ns was used for the above analyses.  
142 While some adjustment to the  $R_g$  occurred at the beginning of equilibration following the anneal  
143 (Supplementary Figure 4), the relative solvent accessibility (RSA) of each monomer type—the  
144 partial SASA normalized by maximum monomer solvation (calculation details in Supplementary  
145 Information)—stabilized quickly (Supplementary Figure 5). It should be noted that the resulting  
146 trends between monomer species follow the aforementioned mobility data, with higher RSA for  
147 monomers which showed greater fluctuations. Unexpectedly, however, monomer RSA is not  
148 strictly correlated to overall chain extension and SASA, with SPMA residues showing significantly  
149 lower accessibility in THF than in water despite adopting a conformation with nearly double the  
150  $R_g$ . If rather than being annealed in organic solvent, the polymers are instead annealed in explicit  
151 water and then transferred to the solvent of interest for equilibration at room temperature, we find  
152 that the same 60 ns is grossly insufficient for full remodeling. After 200 ns, conformations in THF  
153 and DMSO show increased  $R_g$ , though the majority remain far from corresponding equilibrium  
154 values (Supplementary Figure 4). Figure 4 shows more rapid adaptation of RSA at room  
155 temperature, with values trending towards equilibrium for THF and DMSO. Trends towards  
156 equilibrium values indicate that kinetic barriers to rearrangement in THF and DMSO exist but can  
157 be overcome through temperature—as in the annealed simulations—or time, as could be expected  
158 if current trends continued in the room temperature simulations. Contrastingly, in hexane, RSA

159 plateaus before reaching the equilibrium values. While behavior in hexane at room temperature is  
 160 observed to deviate from behavior in water, the assembly remains compact as  $R_g$  maintains values  
 161 below those of the configurations in DMSO and THF. The activation barrier to backbone  
 162 reconfiguration appears to trend with the driving force to compactification, and therefore the  
 163 changes observed in RSA seemingly approach a meta-stable kinetically-trapped state in which  
 164 side-chains have reoriented but the conformation is not entirely reconfigured. The property which  
 165 deviates from the water behavior most quickly at 300 K is the accessibility of SPMA in hexane.  
 166 This rapid change in RSA highlights the high energetic cost of sulfonate exposure to hexane and  
 167 the strong driving force for it to bury within the SCNP core, even if a full remodel is not  
 168 energetically favorable.



169

170 Figure 4. Change in relative solvent accessibility (RSA) of monomers over time after transfer to  
171 solvent of interest at 300 K. Each datapoint shows mean and standard error of the 5 ns average  
172 RSA for each monomer of a given species within the sequence over all conformations. Shaded  
173 regions on the left of each plot show mean RSA from conformations equilibrated in water while  
174 shaded regions on the right of each plot show mean RSA from conformations equilibrated in the  
175 solvent of interest (Supplementary Figure 5).

176 The results presented demonstrate that the covalently bound heterogenous monomers in  
177 our RHP system will lead to compact globules with heterogeneous surfaces in both highly polar  
178 (water) and highly nonpolar (hexane) solvents, though the driving forces differ greatly. The  
179 hydrophobic effect, which drives assembly in water, leads to well solvated polar monomers with  
180 more shielded hydrophobic moieties. In contrast, in hexane, the oleophobic polar and charged  
181 groups avoid exposure and instead bury into the globule core, with hydrocarbon chemistries  
182 prevailing at the assembly's surface. Therefore, the SCNP can exist in drastically different  
183 configurations while still maintaining a compact geometry if the surface energy between the  
184 solvent and monomers is high enough. Contrastingly, if entropic driving forces to polymer motion  
185 outweigh the enthalpic costs to solvent exposure, the chain extends. In DMSO and THF, the  
186 majority of monomers interact favorably with both solvents such that the RHP is generally open  
187 and exposed. SPMA associations can limit extension and motion, but the small quantity of them  
188 in the chain still affords enough freedom for other segments to maintain significant solvation. This  
189 association nonetheless impacts accessibility to SPMA and its neighboring residues to solvent,  
190 which has implications to post-synthetic modification strategies that could be employed. The  
191 equilibrated structures illuminate the potential for interactions between RHPs or amongst RHPs

192 and their environment in various settings, such as during processing in organic solvent to create  
193 self-degrading polyesters or within the hydrophobic interior of cell membranes.<sup>21,27</sup>

194 Beyond equilibrium behavior, our simulations also provide insight into how the polymer  
195 chains get to those unique conformations and could behave upon transfer to distinct environments.  
196 A change in solvent-monomer interaction energies can prompt either unfolding or remodeling,  
197 with some reconfiguration possible without need for expansion to take place. Full reconfiguration  
198 is best achieved using heat to overcome kinetic barriers on simulation timescales, though we also  
199 demonstrated a near immediate adjustment to the new environment without thermal initiation.

200 In summary, the specific chemistry of the monomers selected for a heteropolymer as well  
201 as their interactions with surrounding media prove to be of utmost importance to determining  
202 polymer behavior. The structure which results from a given chemistry can lead to more traditional  
203 SCNPs driven by hydrophobic interactions or other attractive and repulsive forces in certain  
204 conditions while behaving as fully solvated, extended chains in others. The ratios of monomer  
205 chemistries and the solvent polarities can be tailored to make specific moieties—and/or their  
206 neighboring species—accessible or inaccessible. We have shown that reconfiguration can occur  
207 significantly and rapidly with full remodeling possible at room temperature on timescales beyond  
208 those typically accessible in simulation. This observed behavior has profound implications to how  
209 the polymers may fold and assemble as they interface with proteins, surfaces, and other molecules  
210 which impact intramolecular interactions.

## 211 **ASSOCIATED CONTENT**

212 **Supporting Information.** The Supporting Information is available on the **XX** website.

213 Simulation methods, backbone and side-chain mobility, sulfur-potassium RDF, and  $R_g$  over time  
214 (PDF)

215 **AUTHOR INFORMATION**

216 **Corresponding Author**

217 \* aalexand@mit.edu

218 **Funding Sources**

219 This work was supported by the Defense Threat Reduction Agency contract HDTRA11910011.

220 **ACKNOWLEDGEMENTS**

221 We are thankful to Ting Xu and Marco Eres for insightful discussion in the preparation of this  
222 work.

223 **REFERENCES**

224 (1) Alqarni, M. A. M.; Waldron, C.; Yilmaz, G.; Becer, C. R. Synthetic Routes to Single Chain  
225 Polymer Nanoparticles (SCNPs): Current Status and Perspectives. *Macromol. Rapid Commun.*  
226 **2021**, *154* (15), 2100035.

227 (2) Blazquez-martín, A.; Verde-sesto, E.; Moreno, A. J.; Arbe, A.; Colmenero, J. Advances in  
228 the Multi-Orthogonal Folding of Single Polymer Chains into Single-Chain Nanoparticles. **2021**,  
229 1–17.

230 (3) Gao, J.; Le, S.; Thayumanavan, S. Enzyme Catalysis in Non-native Environment with  
231 Unnatural Selectivity Using Polymeric Nanoreactors. *Angew. Chemie Int. Ed.* **2021**.

232 (4) Bhat, R.; Foster, L. L.; Rani, G.; Vemparala, S.; Kuroda, K. The function of peptide-  
233 mimetic anionic groups and salt bridges in the antimicrobial activity and conformation of cationic  
234 amphiphilic copolymers. *RSC Adv.* **2021**, *11* (36), 22044–22056.

- 235 (5) Lamm, R. J.; Pichon, T. J.; Huyen, F.; Wang, X.; Prossnitz, A. N.; Manner, K. T.; White,  
236 N. J.; Pun, S. H. Optimizing the Polymer Chemistry and Synthesis Method of PolySTAT, an  
237 Injectable Hemostat. *ACS Biomater. Sci. Eng.* **2020**, *6* (12), 7011–7020.
- 238 (6) Panganiban, B.; Qiao, B.; Jiang, T.; DelRe, C.; Obadia, M. M.; Nguyen, T. D.; Smith, A.  
239 A. A.; Hall, A.; Sit, I.; Crosby, M. G.; Dennis, P. B.; Drockenmuller, E.; Olvera de la Cruz, M.;  
240 Xu, T. Random heteropolymers preserve protein function in foreign environments. *Science* (80-  
241 ). **2018**, *359* (6381), 1239–1243.
- 242 (7) Yu, W.-H.; Qiu, Z.-L.; Wang, J.-R.; Shen, Y.-J.; Han, J.; Fang, L.-F.; Zhu, B.-K. Novel  
243 nanofiltration membrane prepared by amphiphilic random copolymer nanoparticles packing for  
244 high-efficiency biomolecules separation. *Chem. Eng. J.* **2022**, *430*, 132914.
- 245 (8) Verde-Sesto, E.; Arbe, A.; Moreno, A. J.; Cangialosi, D.; Alegría, A.; Colmenero, J.;  
246 Pomposo, J. A. Single-chain nanoparticles: Opportunities provided by internal and external  
247 confinement. *Mater. Horizons* **2020**, *7* (9), 2292–2313.
- 248 (9) Frisch, H.; Tuten, B. T.; Barner-Kowollik, C. Macromolecular Superstructures: A Future  
249 Beyond Single Chain Nanoparticles. *Isr. J. Chem.* **2020**, *60* (1–2), 86–99.
- 250 (10) Hilburg, S. L.; Ruan, Z.; Xu, T.; Alexander-Katz, A. Behavior of Protein-Inspired  
251 Synthetic Random Heteropolymers. *Macromolecules* **2020**, *53* (21), 9187–9199.
- 252 (11) Scheutz, G. M.; Elgoyhen, J.; Bentz, K. C.; Xia, Y.; Sun, H.; Zhao, J.; Savin, D. A.;  
253 Sumerlin, B. S. Mediating covalent crosslinking of single-chain nanoparticles through  
254 solvophobicity in organic solvents. *Polym. Chem.* **2021**, *12* (31), 4462–4466.

- 255 (12) Zhang, Y. Y.; Jia, X. M.; Shi, R.; Li, S. J.; Zhao, H.; Qian, H. J.; Lu, Z. Y. Synthesis of  
256 Polymer Single-Chain Nanoparticle with High Compactness in Cosolvent Condition: A Computer  
257 Simulation Study. *Macromol. Rapid Commun.* **2020**, *41* (24), 1–7.
- 258 (13) Guazzelli, E.; Masotti, E.; Calosi, M.; Kriechbaum, M.; Uhlig, F.; Galli, G.; Martinelli, E.  
259 Single-chain folding and self-assembling of amphiphilic polyethyleneglycol-modified fluorinated  
260 styrene homopolymers in water solution. *Polymer (Guildf)*. **2021**, *231*, 124107.
- 261 (14) Li, Q.; Constantinou, A. P.; Georgiou, T. K. A library of thermoresponsive PEG-based  
262 methacrylate homopolymers: How do the molar mass and number of ethylene glycol groups affect  
263 the cloud point? *J. Polym. Sci.* **2021**, *59* (3), 230–239.
- 264 (15) Goswami, K. G.; Mete, S.; Chaudhury, S. S.; Sar, P.; Ksendzov, E.; Mukhopadhyay, C.  
265 Das; Kostjuk, S. V.; De, P. Self-Assembly of Amphiphilic Copolymers with Sequence-Controlled  
266 Alternating Hydrophilic-Hydrophobic Pendant Side Chains. *ACS Appl. Polym. Mater.* **2020**, *2* (5),  
267 2035–2045.
- 268 (16) Sadeghi, I.; Asatekin, A. Spontaneous Self-Assembly and Micellization of Random  
269 Copolymers in Organic Solvents. *Macromol. Chem. Phys.* **2017**, *218* (20), 1–9.
- 270 (17) Uddin, M. A.; Yu, H.; Wang, L.; Naveed, K.-R.; Amin, B. U.; Mehmood, S.; Haq, F.;  
271 Nazir, A.; Lin, T.; Chen, X.; Ni, Z. Multiple-stimuli-responsiveness and conformational inversion  
272 of smart supramolecular nanoparticles assembled from spin labeled amphiphilic random  
273 copolymers. *J. Colloid Interface Sci.* **2021**, *585*, 237–249.

- 274 (18) Hattori, G.; Takenaka, M.; Sawamoto, M.; Terashima, T. Nanostructured Materials via the  
275 Pendant Self-Assembly of Amphiphilic Crystalline Random Copolymers. *J. Am. Chem. Soc.* **2018**,  
276 *140* (27), 8376–8379.
- 277 (19) Koda, Y.; Terashima, T.; Sawamoto, M. Multimode Self-Folding Polymers via Reversible  
278 and Thermoresponsive Self-Assembly of Amphiphilic/Fluorous Random Copolymers.  
279 *Macromolecules* **2016**, *49* (12), 4534–4543.
- 280 (20) Matsumoto, K.; Terashima, T.; Sugita, T.; Takenaka, M.; Sawamoto, M. Amphiphilic  
281 Random Copolymers with Hydrophobic/Hydrogen-Bonding Urea Pendants: Self-Folding  
282 Polymers in Aqueous and Organic Media. *Macromolecules* **2016**, *49* (20), 7917–7927.
- 283 (21) DelRe, C.; Jiang, Y.; Kang, P.; Kwon, J.; Hall, A.; Jayapurna, I.; Ruan, Z.; Ma, L.; Zolkin,  
284 K.; Li, T.; Scown, C. D.; Ritchie, R. O.; Russell, T. P.; Xu, T. Near-complete depolymerization of  
285 polyesters with nano-dispersed enzymes. *Nature* **2021**, *592* (7855), 558–563.
- 286 (22) Vao-soongnern, V. Molecular simulation of molecular and surface properties of random  
287 copolymer nanoparticle. *J. Mol. Liq.* **2021**, *342*, 117556.
- 288 (23) Chawathe, M.; Patel, A.; Jonnalagadda, S.; Sidorenko, A. Design of hybrid molecular  
289 brushes with reversible surface adaptability on exposure to specific solvents. *Biointerphases* **2018**,  
290 *13* (4), 041006.
- 291 (24) Buglakov, A. I.; Larin, D. E.; Vasilevskaya, V. V. Orientation- and cosolvent-induced self-  
292 assembly of amphiphilic homopolymers in selective solvents. *Polymer (Guildf)*. **2021**, *232*,  
293 124160.

294 (25) Guazzelli, E.; Martinelli, E.; Galli, G.; Cupellini, L.; Jurinovich, S.; Mennucci, B. Single-  
295 chain self-folding in an amphiphilic copolymer: An integrated experimental and computational  
296 study. *Polymer (Guildf)*. **2019**, *161* (November 2018), 33–40.

297 (26) D.A. Case, I.Y. Ben-Shalom, S.R. Brozell, D.S. Cerutti, T.E. Cheatham, III, V.W.D.  
298 Cruzeiro, T.A. Darden, R.E. Duke, D. Ghoreishi, G. Giambasu, T. Giese, M.K. Gilson, H. Gohlke,  
299 A.W. Goetz, D. Greene, R Harris, N. Homeyer, Y. Huang, S. Izadi, A. Kovalenko, R. Krasny, T.  
300 Kurtzman, T.S. Lee, S. LeGrand, P. Li, C. Lin, J. Liu, T. Luchko, R. Luo, V. Man, D.J.  
301 Mermelstein, K.M. Merz, Y. Miao, G. Monard, C. Nguyen, H. Nguyen, A. Onufriev, F. Pan, R.  
302 Qi, D.R. Roe, A. Roitberg, C. Sagui, S. Schott-Verdugo, J. Shen, C.L. Simmerling, J. Smith, J.  
303 Swails, R.C. Walker, J. Wang, H. Wei, L. Wilson, R.M. Wolf, X. Wu, L. Xiao, Y. Xiong, D.M.  
304 York and P.A. Kollman (2019), AMBER 2019, University of California, San Francisco.

305 (27) Jiang, T.; Hall, A.; Eres, M.; Hemmatian, Z.; Qiao, B.; Zhou, Y.; Ruan, Z.; Couse, A. D.;  
306 Heller, W. T.; Huang, H.; de la Cruz, M. O.; Rolandi, M.; Xu, T. Single-chain heteropolymers  
307 transport protons selectively and rapidly. *Nature* **2020**, *577* (7789), 216–220.

308